Research Paper

Long non-coding RNA LOC100129148 functions as an oncogene in human nasopharyngeal carcinoma by targeting miR-539-5p

Kai-Yu Sun[1], Tao Peng[1], Zhe Chen[1], Peng Song[1], Xu-Hong Zhou[1]

[1] Department of Otorhinolaryngology-Head and Neck Surgery, ZhongNan Hospital, Wuhan University, Wuhan 430071, Hubei, P. R. China

Correspondence to: Xu-Hong Zhou; **email:** xhzwhu@sina.com

Keywords: LOC100129148, hsa-miRNA-539-5p (miR-539-5p), *KLF12*, nasopharyngeal carcinoma (NPC), tumorigenesis
Received: February 15, 2017 **Accepted:** March 11, 2017 **Published:** March 21, 2017

ABSTRACT

Emerging studies have shown that long noncoding RNAs (lncRNAs) play critical roles in carcinogenesis and progression, including human nasopharyngeal carcinoma (NPC). The correlation between lncRNAs expression and NPC development has not been well identified in the recent literature. Recently, high-through put analysis reveals that LOC100129148 is highly expressed in NPC. However, whether the aberrant expression of LOC100129148 in NPC is corrected with tumorigenesis or prognosis has not been investigated. Herein, we identified that LOC100129148 was up-regulated in NPC tissues and cell lines, and higher expression of LOC100129148 resulted in a markedly poorer survival time. Over-expressed LOC100129148 favored, but silenced LOC100129148 hampered cell proliferation in NPC cells. Additionally, LOC100129148 enhanced the KLF12 expression through functioning as a competitive 'sponge' for miR-539-5p. Thus, our study reports a novel mechanism underlying NPC carcinogenesis, and provides a potential novel diagnosis and treatment biomarker for NPC.

INTRODUCTION

Nasopharyngeal carcinoma (NPC), a malignancy of the epithelium that shows a variable degree of squamous differentiation where the vast majority of tumors, are undifferentiated without evidence of keratinization and are typically WHO types II and III [1,2]. Furthermore, the association with Epstein-Barr Virus (EBV) is consistent across all types of NPC although the viral presence may be difficult to demonstrate in those lesions that are WHO type [1,3,4]. Treatment for NPC patients still remains limited to combination of radiotherapy and cytotoxic agents [5]. Therefore, there is a pressing unmet need to expand the current treatment options.

Long noncoding RNAs (lncRNAs) are non-protein-coding transcripts that are > 200 nucleotides in length and reside in the nucleus or cytoplasm [6-8]. LncRNAs plays crucial roles on several systems and might be critical to various types of known cancer genes [8, 10-12]. It has been reported that lncRNAs function as important regulator in NPC. Zou et al reported that ANRIL was up-regulated in NPC and promoted the cancer progression via increasing proliferation, reprograming cell glucose metabolism and inducing side-population stem-like cancer cells [9]. LOC553103 [10], LINC01420 [11], and EWSAT1 [12] also functions as oncogenes in NPC by ceRNAs model Nevertheless, the clinical significance and biological mechanisms of lncRNAs in NPC progression are still remaining largely unknown.

LOC100129148 (NR_033999), a kind of lncRNA located in 7q34, is 463 bp in length (https://www.ncbi.nlm.nih.gov/nuccore/NR_033999). Recently, Yang and his colleagues have reported that LOC100129148 is highly expressed in NPC (4.74-fold than NP tissues) [13], while up to date, there is no related study elaborating the relevance between LOC100129148 expression and NPC progression. The role of LOC100129148 on NPC and its potential biological mechanisms still remain to be explored. Hence, we examined the expression of LOC100129148

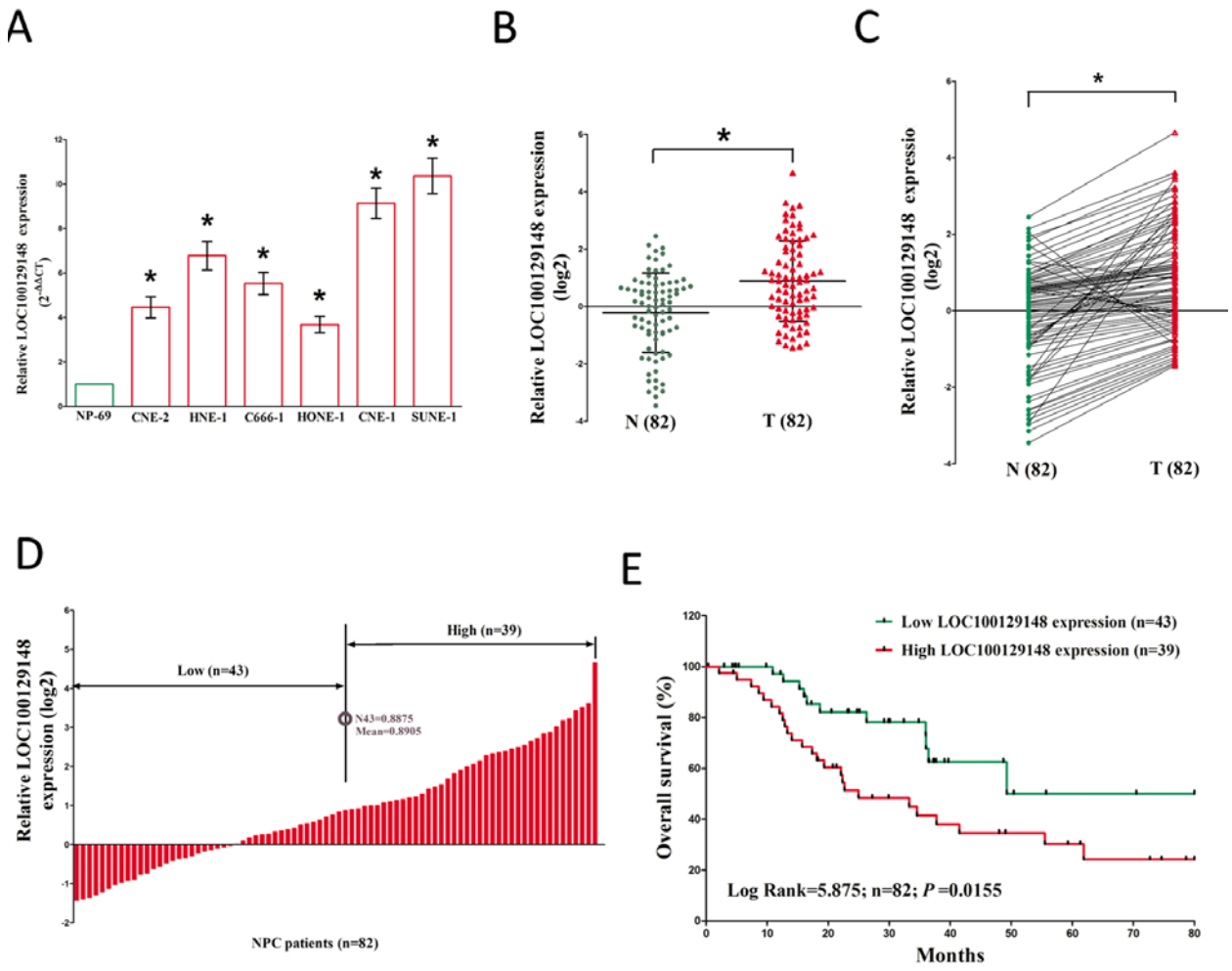

Figure 1. Relative LOC100129148 expression in NPC tissues and cell lines, and its clinical significance. (A) Relative expression of LOC100129148 expression in NPC cell lines and normal NP epidermal cell. **(B)** Relative expression of LOC100129148 expression in NPC tissues (n = 82) and in paired adjacent normal tissues (n = 82). LOC100129148 expression was examined by qPCR and normalized to GAPDH expression. (shown as log2 ∆CT). **(C)** Relative expression of LOC100129148 expression in NPC tissues (n = 82) and in paired adjacent normal tissues (n = 82). LOC100129148 expression was examined by qPCR and normalized to GAPDH expression. (shown as log2 ∆CT). **(D)** NPC patients were divided into a high group (≥mean, n=39) and a low group (<mean, n=43) on the basis of the cutoff value of LOC100129148 expression. **(E)** The Kaplan-Meier survival analysis indicated that LOC100129148 high expression (red line, n=39) has a worse overall survival compared to the low expression subgroup (green line, n=43). **P* < 0.05. Means ± SEM are shown. Statistical analysis was conducted by student t-test.

in NPC tissues cell lines and demonstrated that LOC100129148 might play a critical role in NPC progression and prognosis as a potential prognostic biomarker.

RESULTS

LOC100129148 is over-expressed and associated with prognosis in NPC

To investigate the expression of LOC100129148 in NPC, qRT-PCR was conducted to examine LOC100129148 levels in human NPC tissues and their counterparts. Results revealed that LOC100129148 levels in 82 NPC tissues were significantly lower than that of in 82 counterparts (*P* <0.05) (Fig. 1A-B). Next, we examined LOC100129148 expression in NPC cell lines, and found that LOC100129148 was over-expressed in CNE-2, C666-1, HNE-1, CNE-1, SUNE-1, and HONE-1 cells, compared with that of in NP69 cells (a normal NP cell lines) (Fig. 1C). Among the six NPC cell lines, LOC100129148 are much higher expressed in CNE-1 and SUNE-1 cells, thus, CNE-1 and SUNE-1 cells were chose to conduct the following experiments. Then, NPC patients were divided into a high group (≥ mean, n=39) and a low group (<mean, n=43) on the

basis of the cutoff value of LOC100129148 expression (Fig. 1D). Moreover, Kaplan-Meier analysis indicated that high LOC100129148 expression was related to a poorer OS (log-rank test, P =0.0155, Fig. 1E). These results demonstrated that high LOC100129148 expression was related to poor prognosis, and over-expression of LOC100129148 might be essential in NPC progression.

LOC100129148 promotes growth of NPC cells *in vitro* and *in vivo*

We also studied the impact of LOC100129148 on the proliferation of NPC cells. To this end, CNE-1 and SUNE-1 cells were transfected with control shRNA or shRNAs against LOC100129148, i.e., sh-LOC100129148#1 (sh-1), sh-LOC100129148#2 (sh-2), and sh-LOC100129148#3 (sh-3), pcDNA3.1 control and pcDNA3.1-LOC100129148. The qRT-PCR results indicated that sh-1, sh-2, and sh-3 effectively knocked down LOC100129148, and pcDNA3.1-LOC100129148 significantly increased LOC100129148 expression (Fig. 2A-B).

And then, trypan blue staining, BrdU staining as well as CCK8 assay were conducted to explore the role of LOC100129148 on NPC cell growth, and results demonstrated silence of LOC100129148 induced a reduction in the cell growth of CNE-1 and SUNE-1 cells than that of in their blank counterparts (Fig. 3C, E, and G). However, overexpression of LOC100129148 exhibited a significant increase in the cell growth of CNE-1 and SUNE-1 cells than their blank counterparts (Fig. 3D, F, and H).These results clearly demonstrate that LOC100129148 significantly facilitates cell growth in NPC cells.

To further investigate whether knockdown of LOC100129148 expression could affect tumor growth in vivo, CNE-1 cells stably transfected with sh-1 or shRNA-NC, pcDNA3.1-LOC100129148 or pcDNA3.1-empty vectors were injected into male nude mice. Thirty-six days after inoculation, the tumor size and weight in the sh-1 group were markedly smaller/lighter in comparison to that of in their counterparts group, and the tumor size and weight in the pcDNA3.1-LOC100129148 group was markedly larger/heavier than that of in pcDNA3.1-empty vectors group (Fig. 4A-D). To further investigate the in vivo effects of LOC100129148, tumor cell proliferation was assessed using proliferation-related nuclear antigen Ki67 immunoreactivity assay. We found that up-regulation of LOC100129148 promoted tumor cell proliferation, and down-regulation of LOC100129148 inhibited tumor cell proliferation (Fig. 4E). Taken together, these results demonstrate that LOC100129148 plays a crucial role on NPC progression.

LOC100129148 functions as a ceRNA of miR-539-5p in NPC

Increasing of publications reported lncRNA might function as a ceRNA or a molecular sponge in regulating the biological functions of miRNA. To find miRNAs interacted with LOC100129148, we analyzed the results of miRDB (http://mirdb.org/cgi-bin/custom_predict/customDetail.cgi) to predict potential miRNAs (results were shown in Table 1. In miRDB, miRNAs with target score⩾50 were selected.

To identify which miRNA was the most one that enrich-ment in LOC100129148, we conducted a pull-down assay using a biotin-labeled specific LOC100129148

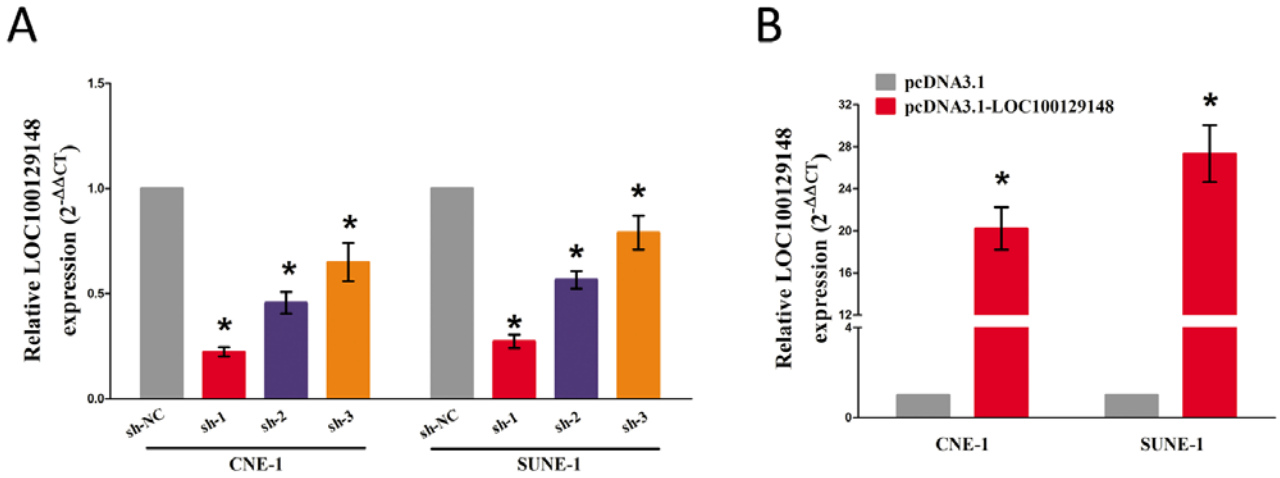

Figure 2. (A-B) Relative LOC100129148 expression after transfection with sh-LOC100129148 or pcDNA3.1-LOC100129148.

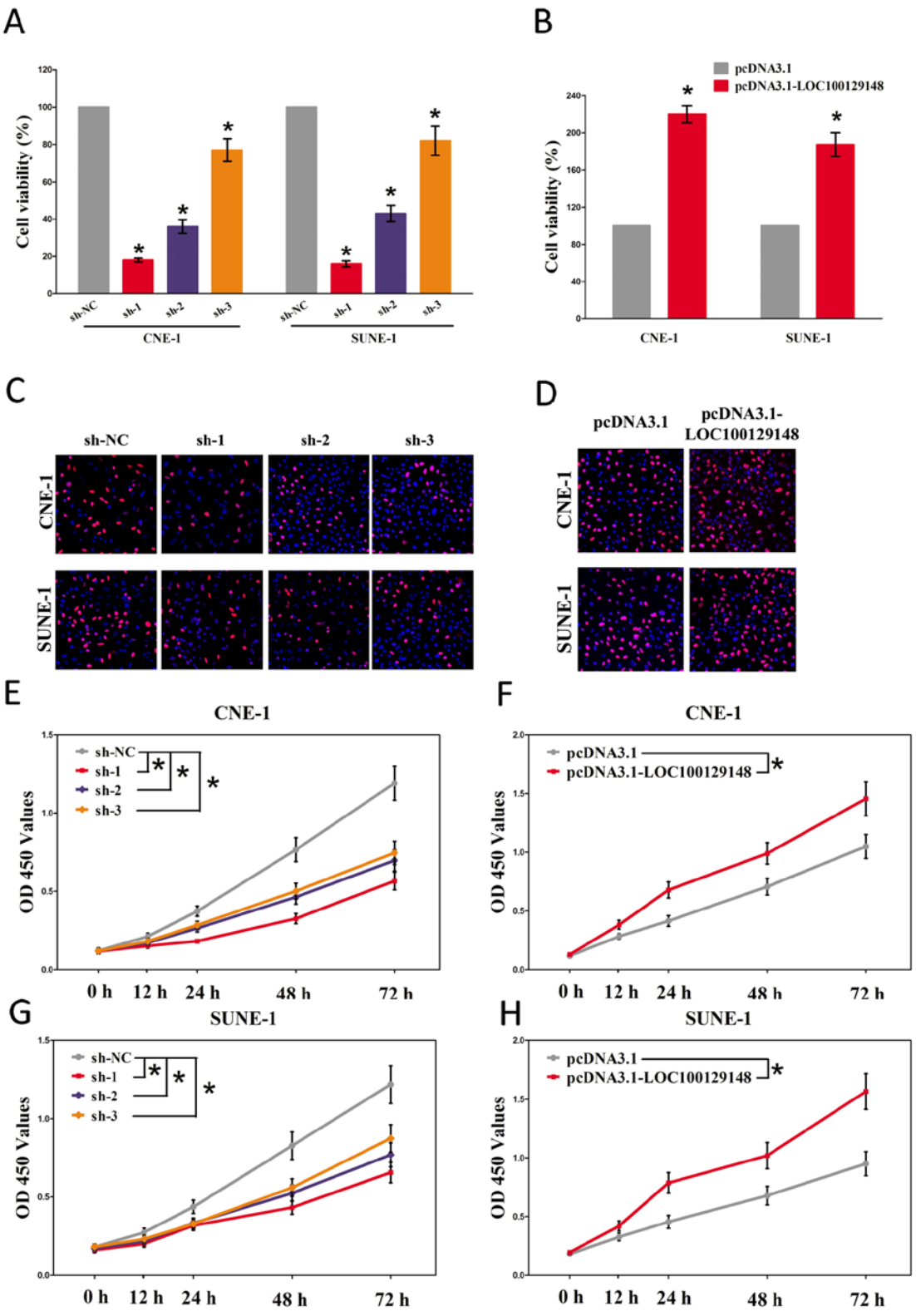

Figure 3. LOC100129148 promotes tumor NPC cell growth *in vitro*. (A-B) Statistical analysis of trypan blue staining. **(C-D)** Shown is representative photomicrograph of BrdU staining assay after transfection for fourteen days. **(E-H)** CCK8 assays of CNE-1 and SUNE-1 cells after transfection. Assays were performed in triplicate. *P < 0.05. Means ± SEM are shown. Statistical analysis was conducted using student t-test.

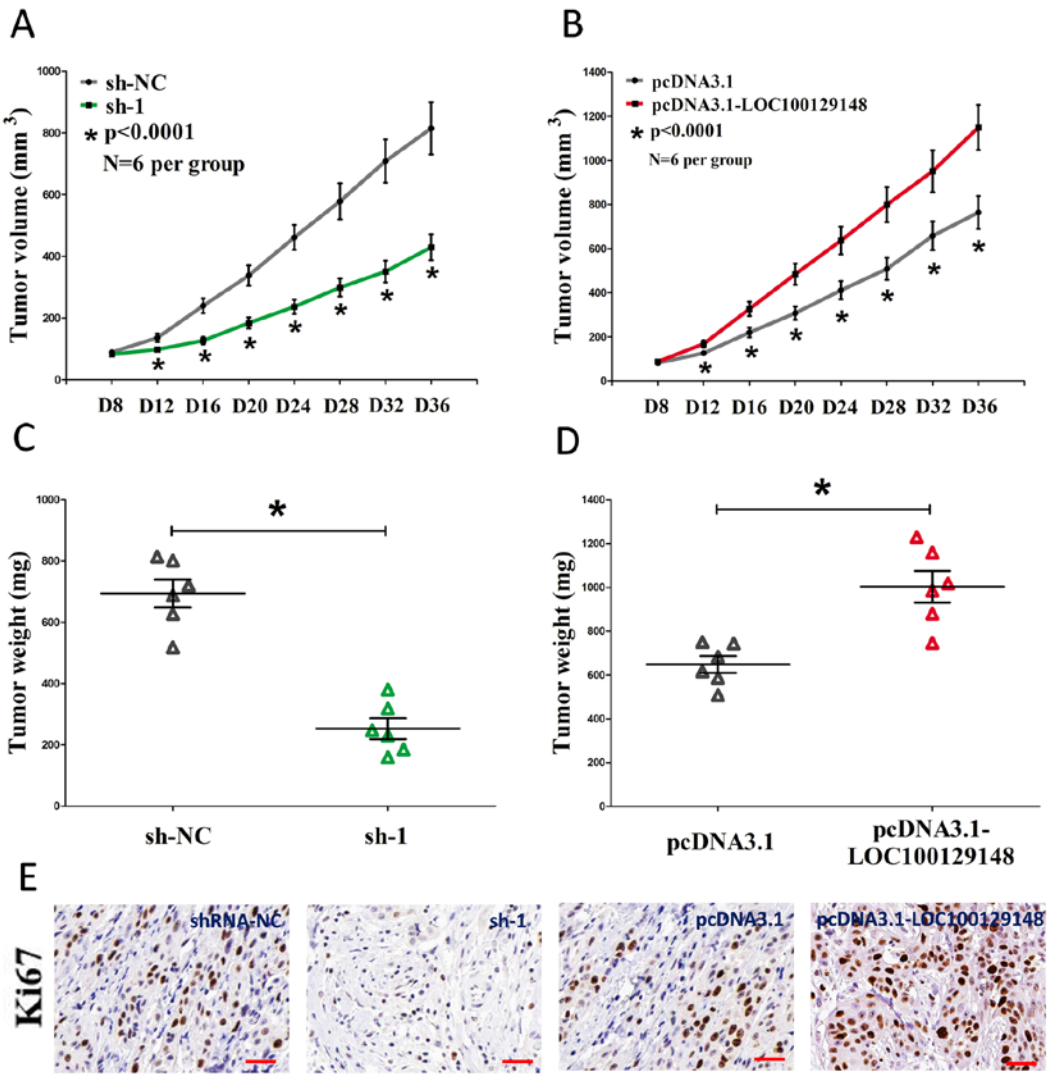

Figure 4. LOC100129148 promotes tumor NPC cell growth in vivo. (A-B) Tumor volume subcutaneous implantation models of CNE-1 cell are shown. **(C-D)** Tumor weight subcutaneous implantation models of CNE-1 cell are shown. **(E)** Immunohistochemistry of Ki67 in tumors isolated from shRNA-NC, sh-1, pcDNA3.1, and pcDNA3.1-LOC100129148 groups. Assays were performed in triplicate. **P* < 0.05. Means ± SEM are shown. Statistical analysis was conducted using student t-test.

Table 1. Predicted results using miRDB (target score≥50).

Target Rank	Target Score	miRNA Name	Gene Symbol
1	92	hsa-miR-539-5p	submission
2	90	hsa-miR-1252-3p	submission
3	77	hsa-miR-6510-5p	submission
4	75	hsa-miR-1227-5p	submission
5	65	hsa-miR-6845-5p	submission
6	65	hsa-miR-6762-5p	submission
7	63	hsa-miR-4640-5p	submission
8	60	hsa-miR-6823-5p	submission
9	55	hsa-miR-4650-3p	submission
10	50	hsa-miR-6771-5p	submission

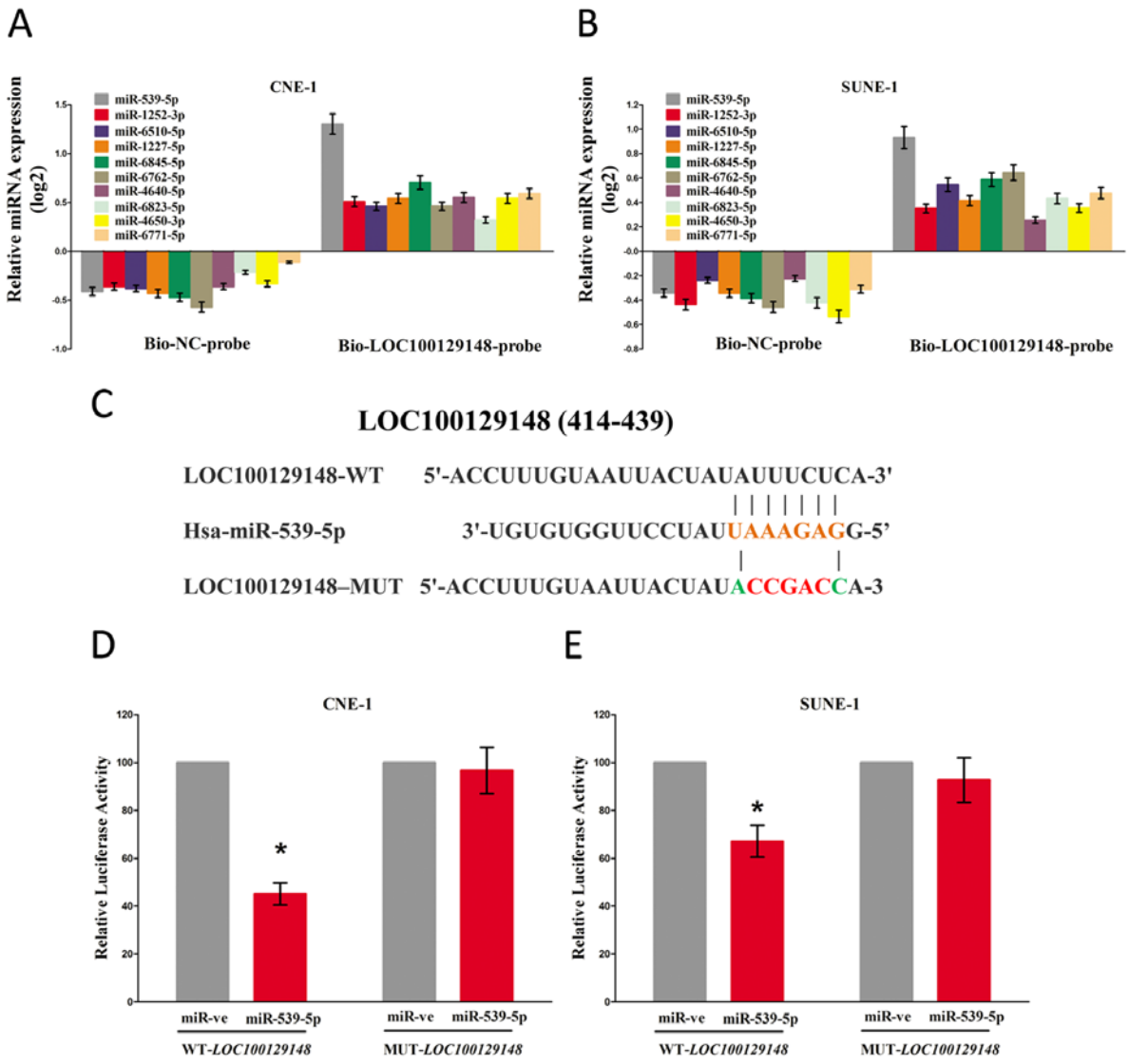

Figure 5. LOC100129148 is a direct target of miR-539-5p. (A-B) Detection of targeted miRNAs using qRT-PCR in the sample pulled down by biotinylated FTH1P3 probe. **(C)** Sequence alignment of miR-539-5p with the putative binding sites within the wild-type regions of LOC100129148. **(D-E)** The luciferase report assay demonstrated that overexpression of miR-539-5p could reduce the intensity of fluorescence in CNE-1 and SUNE-1 cells transfected with the LOC100129148-WT vector, while had no effect on the LOC100129148-MUT vector. Assays were performed in triplicate. **P*< 0.05. Means ± SEM are shown. Statistical analysis was conducted using student t-test.

probe. And a biotin- labeled NC probe was used as a negative control. Then, qRT-PCR was conducted after precipitate. Results revealed that miR-539-5p was much richer in precipitate of LOC100129148 probe than that of in NC probe, and also much richer than that of in other predicted miRNAs (including miR-1252-3p, miR-6510-5p, miR-1227-5p, miR-6845-5p, miR-6762-5p, miR-4640-5p, miR-6823-5p, miR-4650-3p, and miR-6771-5p) (Fig. 5A-B). Moreover, we also conducted dual-luciferase reporter assay to further identify whether LOC100129148 was a functional target for miR-539-5p. Our data demonstrated miR-539-5p may suppress the luciferase activity of pmirGLO-LOC100129148-WT, but it has not affected the luciferase activity of pmirGLO-LOC100129148-MUT (Fig. 5C-E), which implied that miR-539-5p directly bound to LOC100129148 at the recognized sites.

In addition, we also conducted trypan blue staining assay to explore the interaction between miR-539-5p and LOC100129148 on NPC cell growth, and results demonstrated miR-539-5p suppressed cell growth both in CNE-1 and SUNE-1 cells, while when co-transfection of miR-539-5p and pcDNA3.1-LOC100129148,

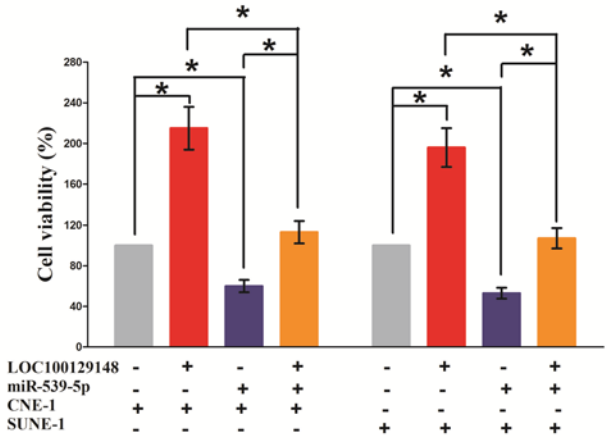

Figure 6. Up-regulated miR-539-5p in CNE-1 and SUNE-1 cells, which stably over-expressed LOC100129148, largely reversed the favorable effects of LOC100129148 on cell proliferation. Assays were performed in triplicate. *P< 0.05. Means ± SEM are shown. Statistical analysis was conducted using student t-test.

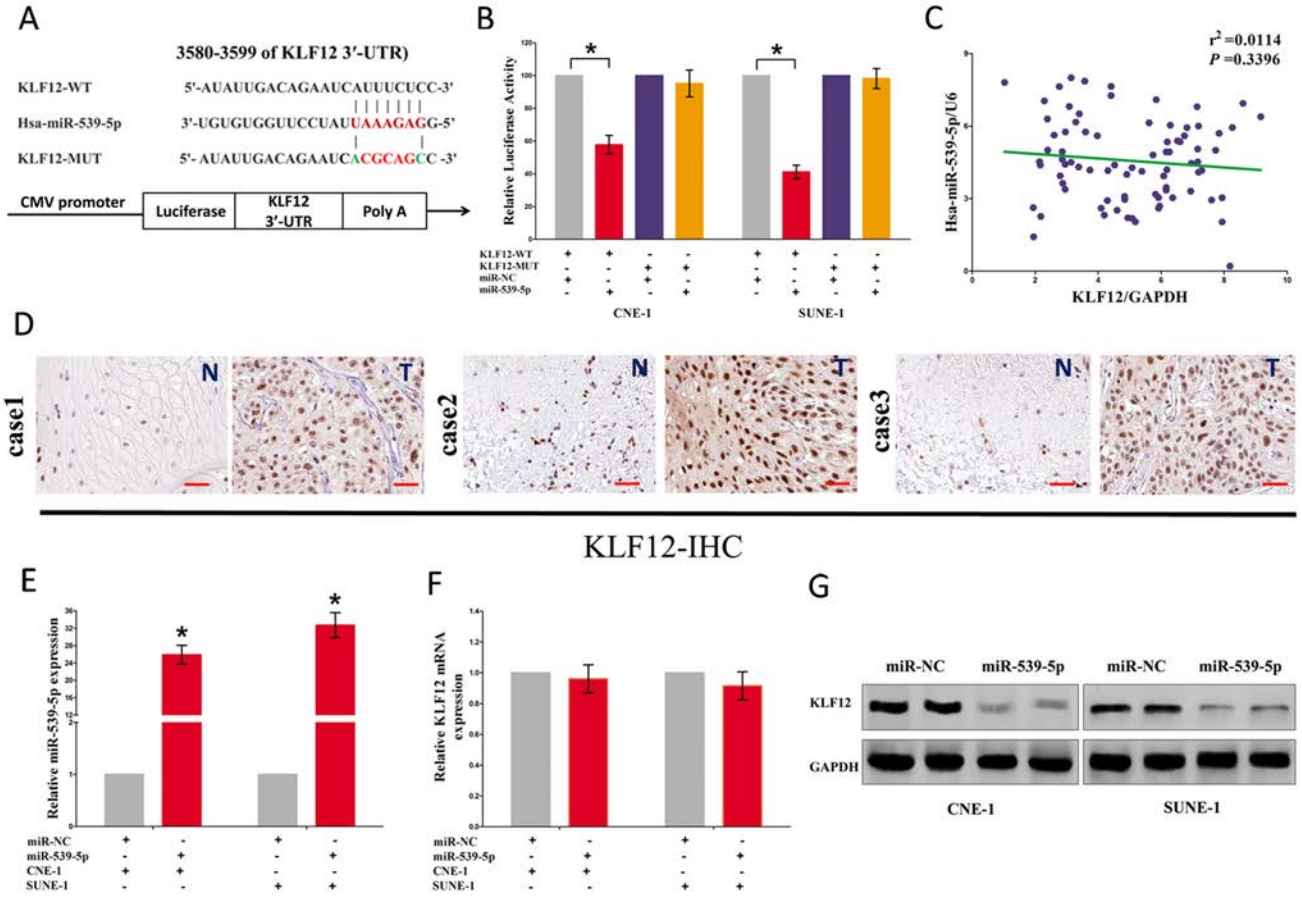

Figure 7. LOC100129148's oncogenic activity is in part through negative regulation of miR-539-5p, and then activation of KLF12 in NPC cells. **(A)** The 3'-UTR of KLF12 harbors one miR-539-5p cognate site. **(B)** Relative luciferase activity of reporter plasmids carrying wild-type or mutant KLF12 3'-UTR in CNE-1 and SUNE-1 cells co-transfected with negative control (NC) or miR-539-5p mimic. **(C)** mRNA expression of KLF12 and miR-539-5p in NPC tissues. **(D)** KLF12 is highly expressed in NPC tissues (T) that NP tissues (N). **(E)** Relative miR-539-5p expression after transfection with miR-NC and miR-539-5p. **(F)** Relative KLF12 mRNA expression after transfection with miR-NC and miR-539-5p. **(G)** Relative KLF12 protein expression after transfection with miR-NC and miR-539-5p. Assays were performed in triplicate. *P < 0.05. Means ± SEM are shown. Statistical analysis was conducted using student One-Way ANOVA test.

the growth-inhibitory role of miR-539-5p was reversed, but the growth expedited role of LOC100129148 was also hampered (Fig. 6). These data demonstrated that LOC100129148 facilitated cell growth via functioning as a ceRNA for miR-539-5p in NPC cell lines.

LOC100129148's oncogenic roles are partially via sponging miR-539-5p, and then activating KLF12

To explore the function of miR-539-5p on NPC, we screen Targetscan, miRanda, PicTar to select potential predicted targets of miR-539-5p. We identified the top 100 potential targets, and among these genes, we found a well-known oncogene, KLF12, which was up-regulated in a large number of malignancies. These revealed that KLF12 could be a direct target of miR-539-5p in NPC (Fig. 7A). Next, we used luciferase reporter assays to verify whether KLF12 expression are really regulated by miR-539-5p, and results demonstrate that miR-539-5p inhibits luciferase activity in CNE-1 cells and SUNE-1 cells at the reporter plasmid with a WT KLF12 3'-UTR, but no significant inhibition was observed at the reporter plasmid with a mutant KLF12 3'-UTR (Fig. 7B). However, our results also demonstrated the mRNA of KLF12 expression had no significant correction with the expression of miR-539-5p in NPC samples (r2 =0.0144, P =0.3396) (Fig. 7C). We also discovered that KLF12 was highly expressed in NPC tissues than that of in normal NP tissues, as demonstrated by IHC assay (Fig. 7D). We also found that transfection with miR-539-5p significantly up-regulated the miR-539-5p expression in CNE-1 and SUNE-1 cells (Fig. 7E). Moreover, miR-539-5p decreased the protein expression but had no influence on the mRNA expression for KLF12 in CNE-1 and SUNE-1 cells (Fig. 7F-G).

We then explored the role and mechanism of miR-539-5p on NPC cell growth. Results of Trypan blue staining revealed miR-5395p treatment suppressed cell growth, and pcDNA3.1-KLF12 treatment facilitated cell growth in CNE-1 and SUNE-1 cells (Fig. 8A). However, when treated CNE-1 and SUNE-1 cells with miR-539-5p plus pcDNA3.1-KLF12, the advantageous role of KLF12 on cell growth was reversed by miR-539-5p, and the growth-inhibitory effect of miR-539-5p was inversed by KLF12 over-expression (Fig. 8A). These data demonstrated that miR-539-5p suppressed cell growth by directly targeting 3'-UTR of KLF12 mRNA. Additionally, pcDNA3.1-LOC100129148 treatment reversed the growth inhibitory effect of sh-KLF12 in CNE-1 and SUNE-1 cells (Fig. 8A), which demonstrated that LOC100129148 facilitated cell growth partially through up regulation of KLF12. Furthermore, we next explored the role of LOC100129148 and miR-539-5p on the protein expression of KLF12. Results demonstrated that both miR-539-5p and sh-KLF12 treatment suppressed protein expression of KLF12, while both pcDNA3.1-LOC100129148 and pcDNA3.1-KLF12 treatment significantly enhanced protein expression of KLF12 in CNE-1 and SUNE-1 cells (Fig. 8B), respectively. However, when treated CNE-1 and SUNE-1 cells with pcDNA3.1-LOC100129148 plus sh-KLF12, the

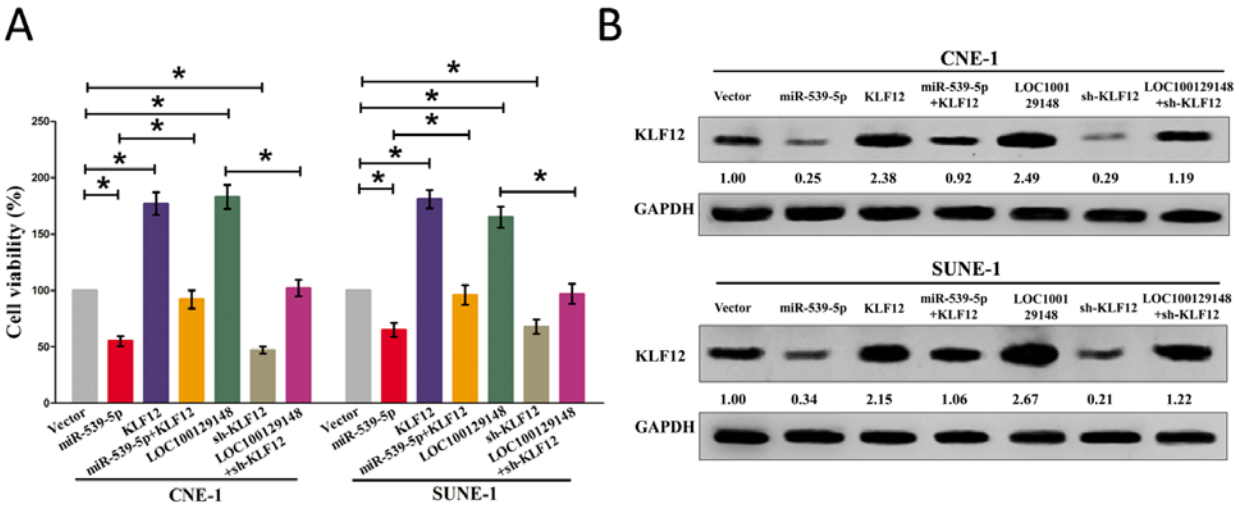

Figure 8. LOC100129148's oncogenic activity is in part through negative regulation of miR-539-5p, and then activation of KLF12 in NPC cells. (A) Statistical analysis of trypan blue staining. **(B)** Protein expression of KLF12 in miR-539-5p, sh-KLF12, LOC100129148, or LOC100129148+sh-KLF12 treated CNE-1 and SUNE-1 cells. Assays were performed in triplicate. *P < 0.05. Means ± SEM are shown. Statistical analysis was conducted using student One-Way ANOVA test.

beneficial role of LOC100129148 on protein expression of KLF12 was suppressed by knockdown of KLF12, and the negative effect of sh-KLF12 was alleviated by over-expression of LOC100129148 (Fig. 8B). These findings suggest that the oncogenic role of LOC100129148 is mediated by miR-539-5p-KLF12 axis in NPC.

DISCUSSION

LncRNAs participate in many biological processes and many studies have implicated that abnormal expression of lncRNAs is closely related to the occurrence and development of malignant tumors [6-8, 10-12, 14-17]. Yang and his colleagues have reported that LOC100129148 is highly expressed in NPC (4.74-fold than NP tissues) [18]. However, the roles and mechanisms of LOC100129148 in NPC have not been well elaborated. Our present study added new evidence that over-expression of LOC100129148 owned oncogenic roles in NPC. LOC100129148 was revealed as a direct target of miR-539-5p, and there was an interactive suppression between them. LOC100129148's function as an oncogene to facilitate tumor progression was partially attributed to its ability to acting as a ceRNA for miR-539-5p, and subsequent to activating of the KLF12 signaling pathway in NPC. Thus, our study contributes to an increasing of literatures supporting the importance of non-annotated lncRNA species in the field of cancer research.

In this study, we reported a novel functional lncRNA LOC100129148 which was significantly high expressed in NPC samples and correlated with a poor prognosis of NPC patients. Our report is the first one to directly explore the association between LOC100129148 expression and NPC. Herein, we found LOC100129148 expression in NPC tissues was significantly higher than that of in NP tissues. Our study also revealed a correction between LOC100129148 levels and NPC prognosis or therapeutic outcome. A strong correction of high LOC100129148 expression in tumors with poor survival was confirmed in 82 NPC samples, revealing that LOC100129148 expression levels could be as a useful prognostic biomarker to help identify patients who are at a higher risk of NPC progression. In addition, LOC100129148 overexpression significantly increased NPC cell viability and growth in vitro, while LOC100129148 knockdown reversed it. In conclusion, our data indicate that LOC100129148 may function as an oncogene and play a critical effect in NPC development and progression.

Although LOC100129148 has been suggested to act as an oncogene, the underlying mechanism by which LOC100129148-mediated gene expression participates in tumorigenesis remains to be clarified. In our present study, we discover the underlying molecular mechanism of LOC100129148 on NPC progression, by functioning as "molecular sponges" to regulate microRNAs. A handle of lncRNAs have been evaluated to play a crucial effect in multiple processes in cells through acting as ceRNAs to regulate microRNAs, including RMRP, NEAT1 [19], and RSU1P2 [20] and so on. MiRNAs play crucial roles in cancers [18, 21-37]. In our study, we investigated the effect of LOC100129148 in NPC cell lines and discovered that LOC100129148 involved in the ceRNA regulatory network and functioned as endogenous miRNA sponges to bind to miR-539-5p and regulated its function. Recent studies indicated miR-539-5p showed tumor suppressive role on osteosarcoma [38], prostate cancer [39], and thyroid cancer [40], while their role on NPC had not been investigated. In our present study, miR-539-5p was decreased expression in NPC tissues and cell lines, and miR-539-5p inhibited growth in NPC cell lines. Moreover, biotin-avidin pull-down system demonstrated LOC100129148 could pull down miR-539-5p. In addition, our study also revealed that miR-539-5p could reverse the favorable roles of LOC100129148 on cell growth in NPC cell lines, which demonstrated LOC100129148 played its favorable role on NPC progression, at least in part, through inhibiting miR-539-5p.

Having shown the critical role of miR-539-5p on suppressing NPC progression, we searched for the potential gene effectors involved in its function. MiR-539-5p can regulate numerous of target genes. Recent study indicated that miR-539 inhibits thyroid cancer cell migration and invasion by directly targeting CARMA1 [40], induces cell cycle arrest in nasopharyngeal carcinoma by targeting cyclin-dependent kinase 4 [41]. MiR-539 inhibits prostate cancer progression by directly targeting SPAG5 [39]. But among all of the predicted target genes for miR-539-5p, we found that KLF12 acted as a crucial effector of miR-539-5p. Aberrant KLF12 expression has been associated to several types of cancers [42, 43]. In our study, highly expression of KLF12 expression was found in NPC than pair-matched adjacent NP tissues. Using bioinformatics, we verified KLF12 as a direct target of miR-539-5p, and luciferase reporter assays confirmed that miR-539-5p targeted KLF12 mRNA at its 3'-UTR. Moreover, our results also demonstrated miR-539-5p exerted its tumor suppressive role on NPC through targeting KLF12. And LOC100129148 facilitated NPC cell growth through up-regulated the expression of KLF12.

In summary, the findings presented in this study suggested that LOC100129148 expression was commonly high expressed in NPC. Furthermore, high

expression of LOC100129148 was an independent poor prognostic for NPC patients. High-expressed LOC100129148 is an oncogenic lncRNA that facilitates the oncogenesis and progression of NPC through miR-539-5p-KLF12 axis. The present results elucidate an underlying mechanism of the oncogenic role for LOC100129148 in NPC, indicating that further investigation of LOC100129148 might lead to the development of novel tumor therapies in NPC.

MATERIALS AND METHODS

Ethical statement

For the analyzed tissue specimens, all patients gave informed consent to use excess pathological specimens for research purposes. The protocols employed in this Subjects Committee. The use of human tissues was approved by the institutional review board of the Wuhan University and conformed to the Helsinki Declaration and to the local legislation. Patients offering samples for the study signed informed consent forms.

Tissue collection

82 cases of fresh NPC tissues and 82 non-cancerous nasopharyngitis (NP) tissues were snap-frozen and stored in liquid nitrogen until further use for qRT-PCR assay. Elective surgery was carried out on these patients at ZhongNan Hospital of Wuhan University (Wuhan, China). The use of tissues for this study has been approved by the ethics committee of ZhongNan Hospital of Wuhan University. Before using these clinical materials for research purposes, all the patients signed the informed consent. None of these patients received any pre-operative chemotherapy or radiotherapy.

Cell Culture and transfection.

The human NPC cell lines, namely, SUNE-1, CNE-1, HNE-1, CNE-2, C666-1 and HONE-1 were cultured in RPMI-1640 (Invitrogen, Carlsbad, CA, USA) supplemented with 10%. fetal bovine serum (FBS). The human immortalized nasopharyngeal epithelial cell line NP69 was cultured in keratinocyte/serum-free medium (Invitrogen) supplemented with bovine pituitary extract. LOC100129148, sh-LOC100129148, miR-539-5p, or sh-KLF12, were purchased from GenePharma Co.,Ltd. (Shanghai, China). Complete medium without antibiotics was used to culture the cells at least twenty-four hours prior to transfection. The cells were washed with 1× PBS (pH7.4) and then transiently transfected with 100 nM NC or LOC100129148, sh-LOC100129148, miR-539-5p , or sh-KLF12, using Lipofectamine™ 2000 (Invitrogen, Carlsbad, CA, USA) according to the manufacturer's instructions.

Western blot

The protein in cells and tissues were extracted using RIPA Lysis Buffer and were separated using SDS-PAGE. After transferred to a PVDF membranes, the membranes were blocked with 5% non-fat milk and incubated with the primary antibodies (Abcam, UK) overnight at 4℃. Then the bands were probed with secondary antibody (Icllab, USA) and visualized by chemiluminescence (Millipore, MA, USA). Rabbit polyclonal antibody against human KLF12 and GAPDH were purchased from Abcam.

EdU assay

For cell proliferation assays, the cells were incubated with 5-ethynyl-20-deoxyuridine (EdU) (Invitrogen, USA) for 5 h, followed by incubation with 300 μl of 1×Apollo® reaction cocktail for 30 min. Then, the DNA contents of the cells were stained with Hoechst 33342 for 30 min and visualized under a fluorescence microscope.

qRT-PCR

Total RNA was extracted with TRIzol reagent in accordance with the manufacturer's instructions (Invitrogen, CA, USA). cDNA was synthesised with the PrimeScript RT reagent Kit (Promega, Madison, WI, USA). Real-time PCR was carried out in a total volume of 10 μl, including 8 μl of TaqMan Power SYBR Green PCR Mix (Invitrogen), 0.5 μl of each primer at 25 μM, and 1 μl of cDNA. The quantitative RT-PCR was carried out on the Roche LightCycler® 96 (LC96) real-time PCR platform using the $2^{-\Delta\Delta CT}$ method. Gene expression results were normalized by internal control GAPDH. Each sample was tested in triplicate.

Immunohistochemistry

Immunohistochemistry of patient tissue sections was performed as described recently [44-46]. The dewaxed 5-μm sections were subjected to an antigen-demasking procedure of brief, high temperature heating of the sections immersed in citrate buffer. Endogenous peroxidases were blocked with 0.3% hydrogen peroxide, and nonspecific binding was blocked with 5% normal goat serum and 2% BSA in phosphate-buffered saline (PBS). Sections were then incubated for 2 hours at room temperature with anti- KLF12 or Ki67 antibody (1:50; Abcam). After washing with PBS, sections were incubated with biotinylated secondary antibody, followed by a further incubation with the streptavidin–

horseradish peroxidase complex. The sections were then immersed in DAB for5 to 10 minutes, counterstained with 10% Mayer hematoxylin, dehydrated, and mounted in crystal mount.

Dual luciferase assay

The putative miR-539-5p target binding sequence in LOC100129148 (KLF12) and its mutant of the binding sites were synthesized and cloned into the downstream of the luciferase gene to generate the wild-type (wt) reporter plasmid and mutated-type (Mut) reporter plasmid. 48 h after transfection, the luciferase activity was measured using the Dual-Luciferase Reporter Assay System (Promega) according to the manufacturer's instructions. The relative luciferase activity was normalized to renilla luciferase activity.

CCK8 Assay

CCK8 Assay was carried out using the protocol described previously [7, 18, 21, 47]. Briefly, cell growth was measured using the cell proliferation reagent WST-8 (Roche Biochemicals, Mannheim, Germany). After plating cells in 96-well microtiter plates (Corning Costar, Corning, NY) at 1.0×10^3 /well, 10 μL of CCK8 was added to each well at the time of harvest, according to the manufacturer's instructions. One hour after adding CCK8, cellular viability was determined by measuring the absorbance of the converted dye at 450 nm.

RNA immunoprecipitation assay

Magna RIP™ RNA-Binding Protein Immunoprecipitation Kit (Millipore, USA) was applied to perform the RIP assay according to the manufacturer's instructions. Whole-cell lysate was harvested and subsequently incubated with RIP buffer containing magnetic beads conjugated with anti-Ago2 antibody (Abcam, UK) or negative control IgG (Sigma-Aldrich, USA). After incubated with Proteinase K, the immunoprecipitated RNA was isolated. The RNA associated with Ago2 antibody was extracted and analyzed by qRT-PCR.

Statistical analysis

All experiments were repeated for three times independently. Results were shown as the means ± standard error mean (SEM). Two independent sample t-test or One-Way Analysis of Variance (ANOVA) was performed using SPSS 20.0 software to assess significant differences in measured variables among groups. A value of P <0.05 was considered to indicate a statistically significant difference.

CONFLICTS OF INTEREST

The authors declare no conflict of interest.

FUNDING

The Fund of the Health and Family Planning of Hubei province, China (NO: WJ2015MB036).

REFERENCES

1. Pathmanathan R, Prasad U, Chandrika G, Sadler R, Flynn K, Raab-Traub N. Undifferentiated, nonkeratinizing, and squamous cell carcinoma of the nasopharynx. Variants of Epstein-Barr virus-infected neoplasia. Am J Pathol. 1995; 146:1355–67.

2. Ke L, Xiang Y, Guo X, Lu J, Xia W, Yu Y, Peng Y, Wang L, Wang G, Ye Y, Yang J, Liang H, Kang T, Lv X. c-Src activation promotes nasopharyngeal carcinoma metastasis by inducing the epithelial-mesenchymal transition via PI3K/Akt signaling pathway: a new and promising target for NPC. Oncotarget. 2016; 7:28340–55. doi: 10.18632/oncotarget.8634.

3. Ozyar E. Prognostic role of negative plasma EBV DNA level in patients with NPC. Oral Oncol. 2016; 63:e7. doi: 10.1016/j.oraloncology.2016.08.011

4. Wu CC, Fang CY, Hsu HY, Chuang HY, Cheng YJ, Chen YJ, Chou SP, Huang SY, Lin SF, Chang Y, Tsai CH, Chen JY. EBV reactivation as a target of luteolin to repress NPC tumorigenesis. Oncotarget. 2016; 7:18999–9017. doi: 10.18632/oncotarget.7967.

5. Bensouda Y, Kaikani W, Ahbeddou N, Rahhali R, Jabri M, Mrabti H, Boussen H, Errihani H. Treatment for metastatic nasopharyngeal carcinoma. Eur Ann Otorhinolaryngol Head Neck Dis. 2011; 128:79–85. doi: 10.1016/j.anorl.2010.10.003

6. Sun CC, Li SJ, Li G, Hua RX, Zhou XH, Li DJ. Long intergenic noncoding RNA 00511 acts as an oncogene in non-small-cell lung cancer by binding to EZH2 and suppressing p57. Mol Ther Nucleic Acids. 2016; 5:e385. doi: 10.1038/mtna.2016.94

7. Sun C, Li S, Zhang F, Xi Y, Wang L, Bi Y, Li D. Long non-coding RNA NEAT1 promotes non-small cell lung cancer progression through regulation of miR-377-3p-E2F3 pathway. Oncotarget. 2016; 7:51784–814. doi: 10.18632/oncotarget.10108.

8. Fang J, Sun CC, Gong C. Long noncoding RNA XIST acts as an oncogene in non-small cell lung cancer by epigenetically repressing KLF2 expression. Biochem Biophys Res Commun. 2016; 478:811–17. doi: 10.1016/j.bbrc.2016.08.030

9. He B, Li W, Wu Y, Wei F, Gong Z, Bo H, Wang Y, Li X, Xiang B, Guo C, Liao Q, Chen P, Zu X, et al. Epstein-Barr virus-encoded miR-BART6-3p inhibits cancer cell metastasis and invasion by targeting long non-coding RNA LOC553103. Cell Death Dis. 2016; 7:e2353. doi: 10.1038/cddis.2016.253

10. Yang L, Tang Y, He Y, Wang Y, Lian Y, Xiong F, Shi L, Zhang S, Gong Z, Zhou Y, Liao Q, Zhou M, Li X, et al. High Expression of LINC01420 indicates an unfavorable prognosis and modulates cell migration and invasion in nasopharyngeal carcinoma. J Cancer. 2017; 8:97–103. doi: 10.7150/jca.16819

11. Song P, Yin SC. Long non-coding RNA EWSAT1 promotes human nasopharyngeal carcinoma cell growth in vitro by targeting miR-326/-330-5p. Aging (Albany NY). 2016; 8:2948–60. doi: 10.18632/aging.101103

12. Zou ZW, Ma C, Medoro L, Chen L, Wang B, Gupta R, Liu T, Yang XZ, Chen TT, Wang RZ, Zhang WJ, Li PD. LncRNA ANRIL is up-regulated in nasopharyngeal carcinoma and promotes the cancer progression via increasing proliferation, reprograming cell glucose metabolism and inducing side-population stem-like cancer cells. Oncotarget. 2016; 7:61741–54. doi: 10.18632/oncotarget.11437.

13. Yang QQ, Deng YF. Genome-wide analysis of long non-coding RNA in primary nasopharyngeal carcinoma by microarray. Histopathology. 2015; 66:1022–30. doi: 10.1111/his.12616

14. Yang D, Lian T, Tu J, Gaur U, Mao X, Fan X, Li D, Li Y, Yang M. LncRNA mediated regulation of aging pathways in Drosophila melanogaster during dietary restriction. Aging (Albany NY). 2016; 8:2182–203. doi: 10.18632/aging.101062

15. Marques Howarth M, Simpson D, Ngok SP, Nieves B, Chen R, Siprashvili Z, Vaka D, Breese MR, Crompton BD, Alexe G, Hawkins DS, Jacobson D, Brunner AL, et al. Long noncoding RNA EWSAT1-mediated gene repression facilitates Ewing sarcoma oncogenesis. J Clin Invest. 2014; 124:5275–90. doi: 10.1172/JCI72124

16. Liu YW, Sun M, Xia R, Zhang EB, Liu XH, Zhang ZH, Xu TP, De W, Liu BR, Wang ZX. LincHOTAIR epigenetically silences miR34a by binding to PRC2 to promote the epithelial-to-mesenchymal transition in human gastric cancer. Cell Death Dis. 2015; 6:e1802. doi: 10.1038/cddis.2015.150

17. Ma MZ, Chu BF, Zhang Y, Weng MZ, Qin YY, Gong W, Quan ZW. Long non-coding RNA CCAT1 promotes gallbladder cancer development via negative modulation of miRNA-218-5p. Cell Death Dis. 2015; 6:e1583. doi: 10.1038/cddis.2014.541

18. Sun C, Sang M, Li S, Sun X, Yang C, Xi Y, Wang L, Zhang F, Bi Y, Fu Y, Li D. Hsa-miR-139-5p inhibits proliferation and causes apoptosis associated with down-regulation of c-Met. Oncotarget. 2015; 6:39756–92. doi: 10.18632/oncotarget.5476.

19. Sun C, Li S, Zhang F, Xi Y, Wang L, Bi Y, Li D. Long non-coding RNA NEAT1 promotes non-small cell lung cancer progression through regulation of miR-377-3p-E2F3 pathway. Oncotarget. 2016; 7:51784–814. doi: 10.18632/oncotarget.10108.

20. Liu Q, Guo X, Que S, Yang X, Fan H, Liu M, Li X, Tang H. LncRNA RSU1P2 contributes to tumorigenesis by acting as a ceRNA against let-7a in cervical cancer cells. Oncotarget. 2016 Jul 26. doi: 10.18632/oncotarget.10844. [Epub ahead of print]

21. Sun C, Liu Z, Li S, Yang C, Xue R, Xi Y, Wang L, Wang S, He Q, Huang J, Xie S, Jiang W, Li D. Down-regulation of c-Met and Bcl2 by microRNA-206, activates apoptosis, and inhibits tumor cell proliferation, migration and colony formation. Oncotarget. 2015; 6:25533–74. doi: 10.18632/oncotarget.4575

22. Sun CC, Li SJ, Li DJ. Hsa-miR-134 suppresses non-small cell lung cancer (NSCLC) development through down-regulation of CCND1. Oncotarget. 2016; 7:35960–78. doi: 10.18632/oncotarget.8482.

23. Sun C, Huang C, Li S, Yang C, Xi Y, Wang L, Zhang F, Fu Y, Li D. Hsa-miR-326 targets CCND1 and inhibits non-small cell lung cancer development. Oncotarget. 2016; 7:8341–59. doi: 10.18632/oncotarget.7071.

24. Sun CC, Li SJ, Zhang F, Pan JY, Wang L, Yang CL, Xi YY, Li J. Hsa-miR-329 exerts tumor suppressor function through down-regulation of MET in non-small cell lung cancer. Oncotarget. 2016; 7:21510–26. doi: 10.18632/oncotarget.7517.

25. Huang J, Sun C, Wang S, He Q, Li D. microRNA miR-10b inhibition reduces cell proliferation and promotes apoptosis in non-small cell lung cancer (NSCLC) cells. Mol Biosyst. 2015; 11:2051–59. doi: 10.1039/C4MB00752B

26. Sun C, Li S, Yang C, Xi Y, Wang L, Zhang F, Li D. MicroRNA-187-3p mitigates non-small cell lung cancer (NSCLC) development through down-regulation of BCL6. Biochem Biophys Res Commun. 2016; 471:82–88. doi: 10.1016/j.bbrc.2016.01.175

27. Sun CC, Li SJ, Yuan ZP, Li DJ. MicroRNA-346 facilitates cell growth and metastasis, and suppresses cell apoptosis in human non-small cell lung cancer by regulation of XPC/ERK/Snail/E-cadherin pathway. Aging (Albany NY). 2016; 8:2509–24. doi: 10.18632/aging.101080

28. Xi Y, Wang L, Sun C, Yang C, Zhang F, Li D. The novel miR-9501 inhibits cell proliferation, migration and activates apoptosis in non-small cell lung cancer. Med Oncol. 2016; 33:124. doi: 10.1007/s12032-016-0837-6

29. Sun CC, Li SJ, Zhang F, Zhang YD, Zuo ZY, Xi YY, Wang L, Li DJ. The novel miR-9600 suppresses tumor progression and promotes paclitaxel sensitivity in non-small-cell lung cancer through altering STAT3 expression. Mol Ther Nucleic Acids. 2016; 5:e387. doi: 10.1038/mtna.2016.96

30. Catapano F, Zaharieva I, Scoto M, Marrosu E, Morgan J, Muntoni F, Zhou H. Altered levels of microRNA-9, -206, and -132 in spinal muscular atrophy and their response to antisense oligonucleotide therapy. Mol Ther Nucleic Acids. 2016; 5:e331. doi: 10.1038/mtna.2016.47

31. Hiraki M, Nishimura J, Takahashi H, Wu X, Takahashi Y, Miyo M, Nishida N, Uemura M, Hata T, Takemasa I, Mizushima T, Soh JW, Doki Y, et al. Concurrent targeting of KRAS and AKT by miR-4689 is a novel treatment against mutant KRAS Colorectal Cancer. Mol Ther Nucleic Acids. 2015; 4:e231. doi: 10.1038/mtna.2015.5

32. Wang H, Bei Y, Huang P, Zhou Q, Shi J, Sun Q, Zhong J, Li X, Kong X, Xiao J. Inhibition of miR-155 protects against LPS-induced cardiac dysfunction and apoptosis in mice. Mol Ther Nucleic Acids. 2016; 5:e374. doi: 10.1038/mtna.2016.80

33. Stiuso P, Potenza N, Lombardi A, Ferrandino I, Monaco A, Zappavigna S, Vanacore D, Mosca N, Castiello F, Porto S, Addeo R, Prete SD, De Vita F, et al. MicroRNA-423-5p promotes autophagy in cancer cells and is increased in serum from hepatocarcinoma patients treated with sorafenib. Mol Ther Nucleic Acids. 2015; 4:e233. doi: 10.1038/mtna.2015.8

34. Chen L, Kang C. miRNA interventions serve as 'magic bullets' in the reversal of glioblastoma hallmarks. Oncotarget. 2015; 6:38628–42. doi: 10.18632/oncotarget.5926.

35. Yu T, Liu L, Li J, Yan M, Lin H, Liu Y, Chu D, Tu H, Gu A, Yao M. MiRNA-10a is upregulated in NSCLC and may promote cancer by targeting PTEN. Oncotarget. 2015; 6:30239–50. doi: 10.18632/oncotarget.4972.

36. Li J, Zhao Y, Lu Y, Ritchie W, Grau G, Vadas MA, Gamble JR. The poly-cistronic miR-23-27-24 complexes target endothelial cell junctions: differential functional and molecular effects of miR-23a and miR-23b. Mol Ther Nucleic Acids. 2016; 5:e354. doi: 10.1038/mtna.2016.62

37. Sun C, Huang C, Li S, Yang C, Xi Y, Wang L, Zhang F, Fu Y, Li D. Hsa-miR-326 targets CCND1 and inhibits non-small cell lung cancer development. Oncotarget. 2016; 7:8341–59. doi: 10.18632/oncotarget.7071.

38. Mirghasemi A, Taheriazam A, Karbasy SH, Torkaman A, Shakeri M, Yahaghi E, Mokarizadeh A. Down-regulation of miR-133a and miR-539 are associated with unfavorable prognosis in patients suffering from osteosarcoma. Cancer Cell Int. 2015; 15:86. doi: 10.1186/s12935-015-0237-6

39. Zhang H, Li S, Yang X, Qiao B, Zhang Z, Xu Y. miR-539 inhibits prostate cancer progression by directly targeting SPAG5. J Exp Clin Cancer Res. 2016; 35:60. doi: 10.1186/s13046-016-0337-8

40. Gu L, Sun W. MiR-539 inhibits thyroid cancer cell migration and invasion by directly targeting CARMA1. Biochem Biophys Res Commun. 2015; 464:1128–33. doi: 10.1016/j.bbrc.2015.07.090

41. Lv LY, Wang YZ, Zhang Q, Zang HR, Wang XJ. miR-539 induces cell cycle arrest in nasopharyngeal carcinoma by targeting cyclin-dependent kinase 4. Cell Biochem Funct. 2015; 33:534–40. doi: 10.1002/cbf.3152

42. Mak CS, Yung MM, Hui LM, Leung LL, Liang R, Chen K, Liu SS, Qin Y, Leung TH, Lee KF, Chan KK, Ngan HY, Chan DW. MicroRNA-141 enhances anoikis resistance in metastatic progression of ovarian cancer through targeting KLF12/Sp1/survivin axis. Mol Cancer. 2017; 16:11. doi: 10.1186/s12943-017-0582-2

43. Du Y, Chen Y, Wang F, Gu L. miR-137 plays tumor suppressor roles in gastric cancer cell lines by targeting KLF12 and MYO1C. Tumour Biol. 2016; 37:13557–69. doi: 10.1007/s13277-016-5199-3

44. Sun C, Yang C, Xue R, Li S, Zhang T, Pan L, Ma X, Wang L, Li D. Sulforaphane alleviates muscular dystrophy in mdx mice by activation of Nrf2. J Appl Physiol (1985). 2015; 118:224–37. doi: 10.1152/japplphysiol.00744.2014

45. Sun CC, Li SJ, Yang CL, Xue RL, Xi YY, Wang L, Zhao QL, Li DJ. Sulforaphane attenuates muscle inflammation in dystrophin-deficient mdx mice via NF-E2-related Factor 2 (Nrf2)-mediated inhibition of NF-kappaB signaling pathway. J Biol Chem. 2015; 290:17784–95. doi: 10.1074/jbc.M115.655019

46. Sun C, Li S, Li D. Sulforaphane mitigates muscle fibrosis in mdx mice via Nrf2-mediated inhibition of TGF-β/Smad signaling. J Appl Physiol (1985). 2016; 120:377–90. doi: 10.1152/japplphysiol.00721.2015

47. Huang CF, Sun CC, Zhao F, Zhang YD, Li DJ. miR-33a levels in hepatic and serum after chronic HBV-induced fibrosis. J Gastroenterol. 2015; 50:480–90. doi: 10.1007/s00535-014-0986-3